

# Experimental and Simulation Study to Identify Current-Confined Path in Cu–Al Space Layer for CPP-GMR Spin-Valve Applications

Joon-Young Soh<sup>1</sup>, Sang-Pil Kim<sup>2,3</sup>, Young Keun Kim<sup>1</sup>, Kwang-Ryeol Lee<sup>4</sup>, Yong-Chae Chung<sup>2</sup>, S. Kawasaki<sup>5</sup>, K. Miyake<sup>5</sup>, M. Doi<sup>5</sup>, and M. Sahashi<sup>5</sup>

<sup>1</sup>Department of Materials Science and Engineering, Korea University, Seoul 136-713, Korea

<sup>2</sup>Division of Advanced Materials Science Engineering, Hanyang University, Seoul 133-791, Korea

<sup>3</sup>Korea Institute of Technology, Seoul, Korea

<sup>4</sup>Korea Institute of Science and Technology, Seoul 136-791, Korea

<sup>5</sup>Department of Electronic Engineering, Tohoku University, Sendai 980-8579, Japan

**To understand the mechanism of current-confined-path formation for the current-perpendicular-to-plane type of giant magnetoresistive devices, we have investigated the evolution of an Al monolayer on the Cu (111) surface both by *in situ* scanning tunneling microscopy and by molecular dynamics simulation. Ultrathin Al nano-clusters were formed on the plateaus and step (or plateau) edges of the Cu surface in the as-deposited state. Upon annealing at 300 °C, Al atoms migrated toward the step edges by surface diffusion. As a consequence, nanometer-sized Cu channels not covered by Al clusters can be formed. These channels could serve as current-confined paths if subsequent mild Al oxidation is provided.**

**Index Terms**—Cu–Al, current-perpendicular-to-plane giant magnetoresistance (CPP-GMR), STM, molecular dynamics.

## I. INTRODUCTION

RECENTLY, the current-perpendicular-to-plane giant magnetoresistance (CPP-GMR) effect has attracted a great deal of interest, because this effect appears best suited for ultra-high-density magnetic storage devices such as read sensors for hard disk drive (HDD) applications. However, the simple metallic CPP-GMR spin-valve sensors are, in general, unable to afford a high degree of sensitivity, because they show small magnetoresistance (MR) ratios with large parasitic resistances. This problem could be solved by the insertion of a nano-oxide layer (NOL) into the Cu spacer of the CPP-GMR spin valves to form a current-confined path (CCP) [1], [2]. Nanometer-sized conductive metallic channels inside the CuAl–NOL are presumed to serve as CCPs that increase the GMR ratio with no appreciable change in the parasitic resistance [3], [4]. However, the details of these nano-channel structures and the method of controlling their size and population remained unclear.

The primary purpose of this study is to examine the mechanism of nano-metallic channel formation in Cu–Al layer structures by *in situ* scanning probe microscopy (SPM) characterization as well as by molecular dynamics (MD) simulation. The latter may serve as a useful process design tool by elucidating the detailed Al atomic cluster construction process on the Cu layer under various energetic conditions, including various atomic impinging energies and temperatures.

## II. EXPERIMENTAL PROCEDURE

The film stack consisted of Ta (5 nm)/Cu (10 nm)/Al (0.2 nm = 1 ML) on a thermally oxidized Si substrate. This

stack was deposited by electro cyclotron resonance (ECR) ion beam sputtering with Xe<sup>+</sup> ions under a base pressure of  $5 \times 10^{-9}$  Torr. Two samples were prepared with and without subsequent *in situ* annealing (300 °C for 30 min), respectively, and both were then subjected to *in situ* oxidation in oxygen ambient at a pressure of  $2.5 \times 10^{-4}$  Torr for 10 min. When the film deposition and surface characterization by reflective high-energy electron diffraction (RHEED) were completed, the film was transported to an SPM chamber ( $1 \times 10^{-10}$  Torr) through a high vacuum transportation module. This SPM chamber is capable of performing atomic force microscopy as well as scanning tunneling microscopy analyses. Therefore, we were able to prevent the surface of the film becoming contaminated throughout the whole experimental processes. The crystal structure of Cu was identified by X-ray diffraction analysis.

## III. MOLECULAR DYNAMICS SIMULATION

To understand the deposition behaviors and the formation of the current channel on an atomic scale, a MD simulation was employed. Empirical interatomic potentials based on the embedded-atom method (EAM) were used in the present simulation. The EAM potentials for Al–Cu system were successfully employed to calculate the physical properties of Al, Cu, and CuAl intermetallic compound [5]. Single-crystal Cu with its (111) surface on top was used as the substrate. In order to fabricate atomic steps on the Cu (111) surface, a 0.5 monolayer (ML) of Cu was deposited on the atomically flat Cu (111) surface. The formation of atomistic steps can be a natural consequence of Cu deposition at room temperature or of the vicinal planes of the Cu (111) surface. The dimension of the substrate area was  $5.6 \times 5.3 \times 1.9 \text{ nm}^3$ , and the *z*-direction was normal to the Cu (111) surface. The kinetic energy of the Al atoms ranged from 0.1 to 3 eV, which is equivalent to that of sputtered atoms

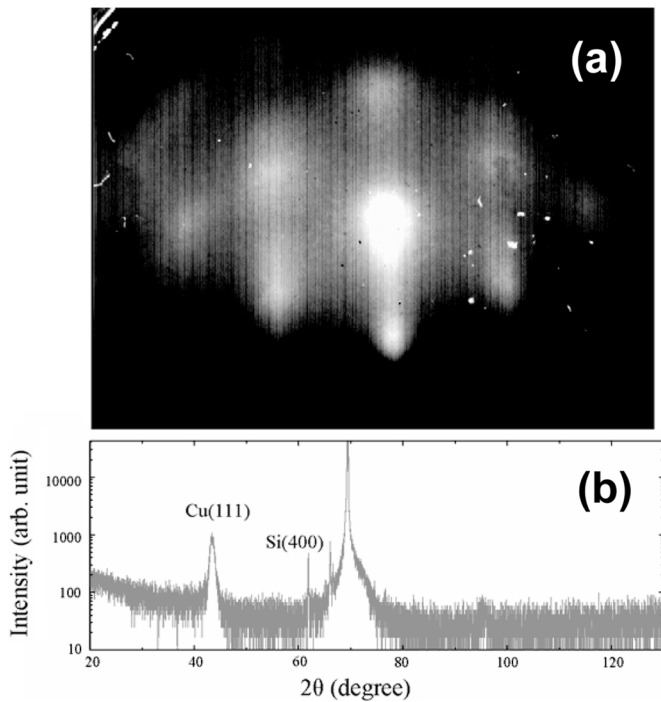


Fig. 1. (a) RHEED pattern of the as-deposited Ta 5-nm/Cu 10-nm surface with an electron beam voltage of 1.8 kV, and (b) XRD pattern of the same surface obtained using Cu  $K\alpha$  radiation where the Cu (111) peak position is  $43.4^\circ$ .

[6], [7]. However, we could not find any significant difference in the surface morphology according to the kinetic energy. Therefore, only the results for the case of 0.1 eV are reported in this paper. The Al atoms were deposited at 300 K (RT) with the incident angle normal to the surface. The lateral position of the deposited atoms was randomly selected. The deposited specimen was annealed at 600 K ( $300^\circ\text{C}$ ) to observe the rearrangement during high-temperature annealing. The XMD 2.5.32 code of Rifkin was used for the molecular dynamics simulation [8].

#### IV. RESULTS AND DISCUSSION

Fig. 1 shows the surface and microstructure of the as-deposited Cu layer characterized by RHEED, and XRD, respectively. Both patterns show that the deposited layer is highly oriented Cu (111). Note that this preferred orientation did not change after annealing at  $300^\circ\text{C}$  for 30 min. According to the AFM measurement (not shown here), this Cu layer possessed a surface roughness (in  $R_a$  value) of 0.34 nm, which became 0.29 nm after annealing. This indicates that the Cu surface was quite smooth, with few steps both before and after annealing. The addition of a 0.5 ML of Al layer is unlikely to alter the roughness values.

A series of *in situ* STM images of the film surfaces is presented in Fig. 2. These data indicates that the surface morphology, in particular that of the surface with an Al layer, changed during the course of annealing.

First, in the as-deposited state, the Al monolayer was formed inhomogeneously in the form of nano-clusters on the Cu (111) surface, because this surface was not perfectly flat. Note that the Cu surface includes 10–30-nm-sized plateau areas, as shown in Fig. 2(a). In addition, the estimated surface roughness (in  $R_a$

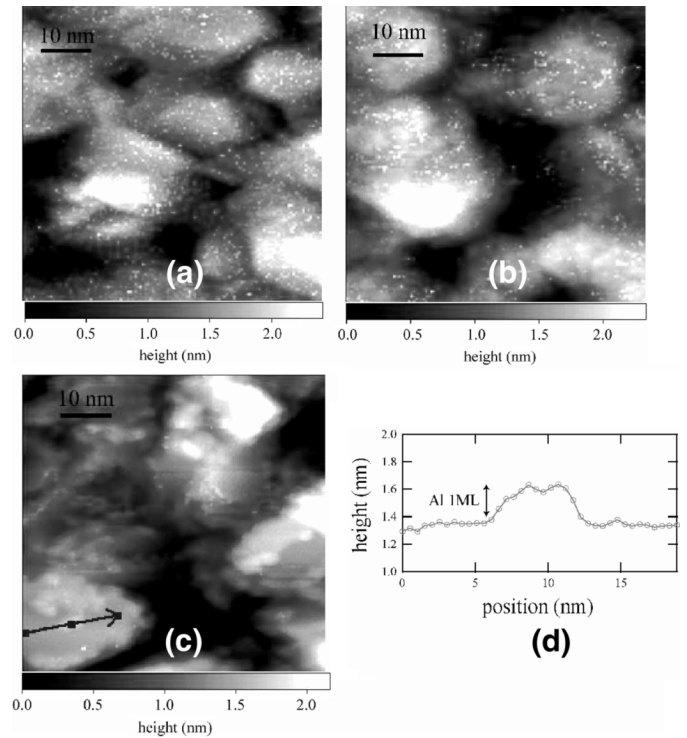


Fig. 2. STM images of (a) Ta 5-nm/Cu 10-nm surface in the as-deposited state where several 10–30-nm-sized plateaus were formed, (b) Ta 5-nm/Cu 10-nm/Al 0.5 ML surface in the as-deposited state, (c) Ta 5-nm/Cu 10-nm/Al 0.5 ML surface after annealing at  $300^\circ\text{C}$ , and (d) line scanning profile of the surface structure. The arrow in the bottom left part of (c) indicates that the size and height of the Al cluster were about 5 and 0.2 nm (or Al 1 ML), respectively. The scanned area was  $60\text{ nm} \times 60\text{ nm}$  for images (a)–(c).

value) of this STM image was 0.383, which is in agreement with the above-mentioned AFM value. Second, the Al atoms migrated to the step edges and segregated there to lower their surface energy upon exposure to annealing. The dimension of the Al clusters is approximately 10 nm, as evidenced by the image in Fig. 2(d). The Cu surface areas that were not covered by Al would be expected to serve as conducting channels, because the subsequent mild natural oxidation does not alter the surface morphology [4].

The molecular dynamics simulation of Al deposition on the Cu (111) surface provided physical insights into the evolution of the thin film structure. Because the surface topography is unvaried by the natural oxidation [4], we focused on the atomic scale configuration of Al atoms on the Cu (111) surface before and after annealing. Fig. 3 shows the surface morphology when Al atoms were deposited on the roughened Cu (111) surface. The MD simulation showed that the deposited Al atoms possessed high mobility on the Cu (111) surface even at room temperature. This high mobility is due to the low-energy barrier between the fcc and hcp sites on the surface. Hence, the Al atoms deposited on the terrace (bottom portion of the Cu surface) tend to segregate to the steps that are energetically the most favorable sites. The segregation of the Al atoms to the steps is evident in Fig. 3(a) and (b). On the other hand, those Al atoms that arrived on the topmost plateau remained there because of the so-called Ehrlich–Schwoebel (ES) barrier near the step-edge that prevents the deposited atoms from descending to the lower terrace [8], [9].

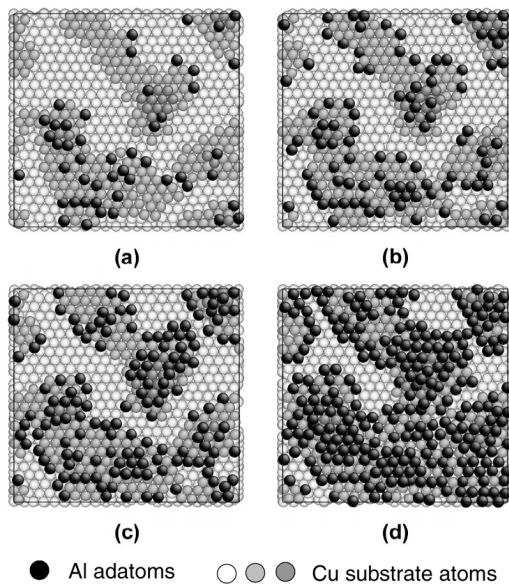


Fig. 3. Molecular dynamics simulation results: The snapshot indicates the behavior of the Al atoms on the Cu (111) surface after the deposition of (a) 50, (b) 100, (c) 150, and (d) 264 (0.5 ML) Al atoms. The black circles are the deposited Al atoms while the white ones are the Cu substrate atoms, and the gray ones represent the Cu atoms in the plateau regions.

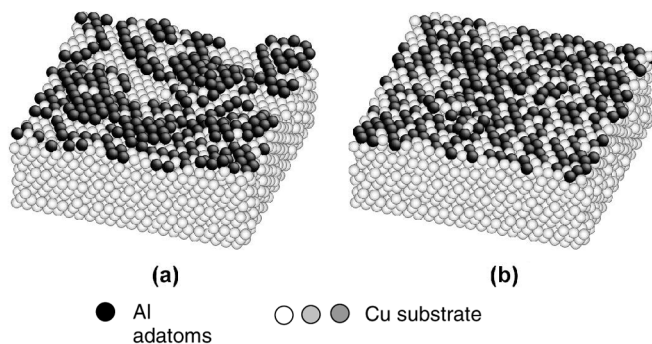


Fig. 4. Atomic configurations of Cu/Al (0.5 ML): (a) as-deposited and (b) after annealing at 600 K. The black circles are the deposited Al atoms and the white circles are the Cu substrate atoms.

Even though the deposition positions of the Al atoms are random, the Al distribution on the surface is rather inhomogeneous, as can be seen in Fig. 4(d). This result is, at least qualitatively, in agreement with the STM observation. The present simulation shows that the inhomogeneity of the surface feature originates from the high mobility of the Al atoms on the Cu (111) surface.

Thermal annealing at 600 K significantly changed the microstructures. Fig. 4 shows the change in the surface morphology of the 0.5 ML Al-deposited structure induced by thermal annealing at 600 K. Three phenomena were observed during thermal annealing. First, the Al atoms situated on top of the plateau descended down to the lower terrace, because their thermal energy was sufficient to overcome the ES barrier.

Second, a significant amount of atomic intermixing occurred between Cu and Al, as evidenced by the more uniform Cu–Al alloyed layer that was observed on the surface. Finally, the Cu atomic steps decreased in size due to active exchange between the substrate Cu atoms. Consequently, the thermal annealing results in the formation of a smooth and homogeneous Cu–Al surface layer. The homogeneous distribution of the Al atoms afforded by the thermal annealing would result in finer conducting channels upon the formation of Al nano-oxide layers.

## V. CONCLUSION

Both experimental and simulation techniques were employed to study the mechanism of Cu conducting channel formation in the Cu–Al space layer system. The Al atoms deposited on the Cu (111) surface showed active surface diffusion behavior and covered the Cu surface with nanometer-sized Al atomic clusters. Annealing at elevated temperatures induced Al segregation at the Cu surface step edges. The MD simulation offered valuable insights into the surface evolution observed by STM measurements. Though it would require intensive computational capability, and a longer computation time, a future study involving a larger area (at least  $20 \text{ nm} \times 20 \text{ nm}$ ) would be useful to compare experimental details more directly.

## ACKNOWLEDGMENT

This work was supported by Grant Number M60 501 000 045-05A0100-04 510 from the International Collaborative Research Program of the Korea Science and Engineering Foundation, and by Grant Number M10 500 000 105-05J0000-10 510 from the National Research Laboratory Program of the Korea Science and Engineering Foundation. This work was also supported by Core Capability Enhancement Program (V00910) of Korea Institute of Science and Technology, and by Industrial Technology Research Grant Program in 2006 from New Energy and Industrial Technology Development Organization (NEDO) of Japan.

## REFERENCES

- [1] M. Takagishi, K. Koi, M. Yoshikawa, T. Funayama, H. Iwasaki, and M. Sahashi, *IEEE Trans. Magn.*, vol. 38, pp. 2277–2282, 2002.
- [2] H. Fukuzawa, H. Yuasa, S. Hashimoto, K. Koi, H. Iwasaki, M. Takagishi, Y. Tanaka, and M. Sahashi, *IEEE Trans. Magn.*, vol. 40, pp. 2236–2238, 2004.
- [3] H. Fukuzawa, H. Yuasa, S. Hashimoto, H. Iwasaki, and Y. Tanaka, *Appl. Phys. Lett.*, vol. 87, pp. 082 507 (1)–082 507 (3), 2005.
- [4] S. Kawasaki, J. Soh, K. Miyake, M. Doi, and M. Sahashi, *J. Magn. Soc. Jpn.*, vol. 30, pp. 357–360, 2006.
- [5] J. Cai and Y. Y. Ye, *Phys. Rev. B*, vol. 54, pp. 8389–8410, 1996.
- [6] M. V. R. Murty, *Surf. Sci.*, vol. 500, pp. 523–544, 2002.
- [7] R. V. Stuart, G. K. Wehver, and G. S. Anerson, *J. Appl. Phys.*, vol. 40, p. 803, 1969.
- [8] J. Rifkin, “XMD Molecular Dynamics Program,” Center for Materials Simulation, University of Connecticut, Storrs, CT, 2002.
- [9] G. Ehrlich and F. G. Hudda, *J. Chem. Phys.*, vol. 44, p. 1039, 1966.
- [10] R. L. Schwoebel, *J. Appl. Phys.*, vol. 40, p. 614, 1969.